Drug and Alcohol Dependence 233 (2022) 109353

Contents lists available at ScienceDirect

Drug and Alcohol Dependence

journal homepage: www.elsevier.com/locate/drugalcdep

Cue-induced craving and negative emotion disrupt response inhibition in methamphetamine use disorder: Behavioral and fMRI results from a mixed Go/No-Go task

Amirhossein Dakhili [a,b,1], Arshiya Sangchooli [c,1], Sara Jafakesh [d], Mehran Zare-Bidoky [c,e], Ghazaleh Soleimani [f], Seyed Amir Hossein Batouli [g], Kamran Kazemi [d], Ashkan Faghiri [h], Mohammad Ali Oghabian [a,i], Hamed Ekhtiari [j,*]

[a] Neuroimaging and Analysis Group. (NIAG), Research Center for Molecular and Cellular Imaging, Tehran University of Medical Sciences, Tehran Iran
[b] Medical Physics Department, Iran University of Medical Sciences, Tehran, Iran
[c] Iranian National Center for Addiction Studies (INCAS), Tehran University of Medical Science, Tehran, Iran
[d] Department of Electrical and Electronics Engineering, Shiraz University of Technology, Shiraz, Iran
[e] School of Medicine, Shahid-Sadoughi University of Medical Sciences, Yazd, Iran
[f] Department of Biomedical Engineering, Amirkabir University of Technology (Tehran Polytechnic), Tehran, Iran
[g] Department of Neuroscience and Addiction Studies, School of Advanced Technologies in Medicine, Tehran University of Medical Sciences, Tehran, Iran
[h] Tri-Institutional Center for Translational Research in Neuroimaging and Data Science (TReNDS), Georgia State University, Georgia Institute of Technology, and Emory University, Atlanta, GA 30303, USA
[i] Medical Physics and Biomedical Engineering Department, Tehran University of Medical Sciences, Tehran Iran
[j] Laureate Institute for Brain Research (LIBR), Tulsa, OK, USA

ARTICLE INFO

Keywords:
Methamphetamine
FMRI
Cue reactivity
Craving
Response inhibition
Go/No-Go

ABSTRACT

Background: Drug-related cue-reactivity, dysfunctional negative emotion processing, and response-disinhibition constitute three core aspects of methamphetamine use disorder (MUD). These phenomena have been studied independently, but the neuroscientific literature on their interaction in addictive disorders remains scant.
Methods: 62 individuals with MUD were scanned when responding to the geometric Go or No-Go cues superimposed over blank, neutral, negative-emotional and drug-related background images. Neural correlates of drug and negative-emotional cue-reactivity, response-inhibition and their interactions were estimated, and methamphetamine cue-reactivity was compared between individuals with MUD and 23 healthy controls. Relationships between behavioral characteristics and observed activations were investigated.
Results: Individuals with MUD had longer reaction times and more errors in drug and negative-emotional compared to blank blocks, and more omission errors in drug compared to neutral blocks. They showed higher drug cue-reactivity than controls across prefrontal, fusiform, and visual regions ($Z > 3.1$, p-corrected<0.05). Response-inhibition was associated with precuneal, inferior parietal, anterior cingulate, temporal, and inferior frontal activations ($Z > 3.1$, p-corrected<0.05). Response-inhibition in drug cue blocks coincided with higher activations in the visual cortex and lower activations in the paracentral lobule and superior and inferior frontal gyri, while inhibition during negative-emotional blocks led to higher superior parietal, fusiform, and lateral occipital activations ($Z > 3.1$, p-corrected<0.05).
Conclusion: Drug cue-reactivity may impair response inhibition partly through activating dis-inhibitory regions, while temporal and parietal activations associated with response-inhibition in negative blocks suggest compensatory activity. Results suggest that drug and negative-emotional cue-reactivity influence response-inhibition, and the study of these interactions may aid mechanistic understanding of methamphetamine use disorder.

* Correspondence to: Laureate Institute for Brain Research, 6655 South Yale Ave, Tulsa, OK 74136, USA.
E-mail address: hekhtiari@laureateinstitute.org (H. Ekhtiari).
[1] Contributed equally to the manuscript as first authors.

https://doi.org/10.1016/j.drugalcdep.2022.109353
Received 21 August 2021; Received in revised form 7 February 2022; Accepted 9 February 2022
Available online 11 February 2022

1. Introduction

Methamphetamine is the most common amphetamine-type stimulant, with increasing use around the globe (United Nations Office on Drugs and Crime, 2018). The prevalence of methamphetamine use disorder (MUD) in the US has increased by 195% between 2010 and 2018, with a 200% increase in deaths due to overdose from 2011 to 2016, leading some to suggest that it might be responsible for the next substance use crisis in the US (Hedegaard et al., 2018). Evidence suggests that MUD involves a constellation of neuro-cognitive changes which cause and sustain addictive behavior, with three prominent themes emerging from the literature: Individuals with MUD are overly sensitized to stimuli associated with methamphetamine use through aberrant positive reinforcement, with a heightened activation of the reward network and associated brain regions in response to methamphetamine cues (Alam Mehrjerdi et al., 2011; Ekhtiari et al., 2020); they may have difficulties regulating negative emotions and associate methamphetamine with relief, with MUD instituted through negative reinforcement (May et al., 2020); and they typically have difficulties in response-inhibition, which may contribute to methamphetamine use and relapse after other processes (such as methamphetamine cues or negative emotional states) induce methamphetamine craving and a shift to a drug-seeking neuro-cognitive state (Monterosso et al., 2005; Nestor et al., 2011).

Interestingly, these three domains might be relevant across substance use disorders (SUDs): The Addictions Neuroclinical Assessment (ANA) model is based around the three domains of incentive salience, negative emotionality, and executive function (Kwako et al., 2017); the impaired response-inhibition and salience attribution (iRISA) model of addiction centers problematic cognitive control over substance use and the misattribution of high salience to substance-related rewards (Goldstein and Volkow, 2002, 2011); and there is broad consensus that the cognitive control, positive valence and negative valence research domain criteria (RDoC) are uniquely crucial in SUDs, with drug cue-reactivity notably absent in RDoC (Yücel et al., 2019). Using behavioral tasks to engage response-inhibition, negative emotion processing and drug cue-reactivity, a growing cognitive neuroscience literature has painted a complex pattern of neural activity underlying the dysfunctions in these domains. Impairments of inhibitory control, assessed using paradigms such as the Go/No-Go task (Luijten et al., 2014), are associated with different activation patterns in SUDs compared to healthy controls (HCs) in the supplementary motor area, insula, precuneus, and many temporal and frontal regions (Kelly et al., 2004; Mostofsky et al., 2003; Nestor et al., 2011; Paulus et al., 2005; Simmonds et al., 2008). Drug cue-reactivity, the host of behavioral, physiological and neural responses to drug cues which are associated with a cue-induced craving for addictive substances and subsequent drug use behavior (Ekhtiari et al., 2021), is associated with activations across the frontal, insular, striatal and limbic regions, overlapping those involved in dysfunctional response-inhibition (Dean et al., 2019; Grodin et al., 2019; Guterstam et al., 2018; Yin et al., 2012; Zilverstand et al., 2018).

While most task-based fMRI studies of SUDs have examined these phenomena separately, contextual response-inhibition might be more relevant in addictive disorders compared to general response-inhibition. Increasing evidence suggests that exposure to drug or alcohol cues can impair response-inhibitory performance and higher error rates (Jones et al., 2018; Su et al., 2020) and a range of negative affects can lead to disinhibition (Curci et al., 2013; Cyders and Coskunpinar, 2011; Cyders and Smith, 2008), suggesting that response-inhibitory processes may be impacted by contextual stimuli. This influence can be viewed as reflecting “negative urgency” and “positive urgency”– impulsivity during experiences of negative and positive affect – which, notably, might be better predictors of addictive behaviors than general impulsivity (Cyders and Smith, 2008; Kaiser et al., 2012). This has led to some recent fMRI investigations utilizing variants of the Go/No-Go task to contrast neural activity associated with response-inhibition during exposure to neutral, drug, and negative cues, revealing distinct activation patterns which suggest increased neural inhibitory load (Ames et al., 2014; Czapla et al., 2017; Stein et al., 2021).

The present study is the first to investigate the neural substrates of response-inhibition during drug cue-reactivity and negative emotional cue-reactivity in MUD, using a novel fMRI task that combines a Go/No-Go task with drug cue-reactivity and negative emotional cue-reactivity paradigms. A major advantage compared to several previous studies of response-inhibition during drug cue-reactivity (Ames et al., 2014; Czapla et al., 2017) is that, similar to Stein et al. (2021), we use different cues for the Go/No-Go conditions than drug and negative cues, allowing for a fully factorial investigation of the neural correlates of drug cue-reactivity, negative cue-reactivity, response-inhibition, and response-inhibition during drug and negative cue-reactivity. Another divergence from most prior literature is our inclusion of both drug and negative affective cues in the task, which has been attempted for gambling disorder but not any SUDs (van Holst et al., 2012). We hypothesize that individuals with MUD will perform more poorly in the Go/No-Go task when exposed to methamphetamine-related and negative cues than neutral cues, and that exposure to these cues would modulate the brain activity associated with response-inhibition. We also investigate associations between behavioral and clinical measures and the neural correlates of contextual response-inhibition to assess the potential relevance of contrasts estimated using the task.

2. Materials and methods

2.1. Participants

Male participants with MUD, aged 20–40 years, were recruited from multiple addiction treatment centers in Tehran, Iran. All participants met the following inclusion criteria: (1) Diagnosis of methamphetamine dependence (for at least six months) according to the Diagnostic Statistical Manual of Mental Disorders, Fourth Edition, Text Revision (American Psychiatric Association, 2013), (2) abstinence from any substance except nicotine for at least a week, confirmed by negative urine drug screening and self-report, (3) right-handedness, as determined using the Edinburgh Handedness Inventory (Oldfield, 1971). Exclusion Criteria were: (1) comorbid axis-I disorders, other than drug dependence (According to DSM-IV-TR), (2) ineligibility for MRI scanning (e.g., metal implants, claustrophobia), (3) head trauma with neurologic sequelae, 4) neurologic disorder which interferes with the research process. Written informed consent was obtained from all participants. A total of 75 individuals with MUD were screened in the laboratory. Thirteen did not meet inclusion criteria, leaving 62 participants who enrolled and completed the entire protocol. Nine individuals with MUD were excluded from data analysis due to high head motion during scanning, leaving a total of 53 individuals with MUD for fMRI analyses.

To validate the drug cue-reactivity aspect of the task, 23 healthy individuals were chosen as HCs. The HCs had no past or current diagnosis of substance use disorder or history of methamphetamine use and otherwise had the same inclusion and exclusion criteria as Those with MUD.

The study was conducted in accordance with the Declaration of Helsinki. Individuals with MUD were told that the fMRI task could induce methamphetamine craving and they would be asked to remain in the scanning center for an hour to recover. Participants then provided written, informed consent prior to further screening for enrollment. All collected data were anonymized by the data analyst before further analysis. The study protocol was approved by the ethical review board of the Tehran University of Medical Sciences with the approval code 93–02–98–23869.

2.2. Measures and questionnaires

Potential participants were assessed by two clinical psychologists. Several questions and measures were administered before scanning, including demographic information, the Barratt Impulsiveness Scale-11 (BIS-11) (Barratt, 1994) and the Depression Anxiety and Stress Scale-21 (DASS-21) (Osman et al., 2012). A Drug Abuse Profile instrument was used to assess participant history of treatment for substance use disorders; total drug abuse duration; total abstinence duration; and the number of days on which participants abused methamphetamine, cannabis, alcohol, sedatives, hallucinogens (including LSD, psilocybin mushrooms and MDMA), cocaine, opioids (heroin and crack heroin, opium, poppy milk, buprenorphine, diphenoxylate, tramadol and norgesic) in the last 30 days before the start of treatment. A Risky Behaviors Profile instrument was utilized to assess the history of injecting drug use, high-risk sexual behavior, incarceration, drug selling, and physical altercation (Supplementary materials). Before and after scanning, individuals with MUD also rated their drug craving on a 0–100 Visual Analog Scale (VAS), with the question "how much craving are you experiencing right now?". Participants also rated their positive and negative affective experiences using a positive and negative scale (PANAS) (Crawford and Henry, 2004), before and after scanning.

2.3. Mixed Go/No-Go task

All individuals with MUD and HCs were scanned during four consecutive runs of the mixed Go/No-Go task, separated by resting blocks with a fixation point. Each run consisted of four 36-second blocks, each containing 24 pictures depicting geometric Go/No-Go stimuli superimposed on the background cues. Background images were either blank, neutral cues, negative cues, and drug cues. The order of the blocks was pseudo-randomized in each run. The 24 drug-related cues have been evaluated in previous studies (Ekhtiari et al., 2010) and the neutral and negative cues were selected from the International Affective Picture

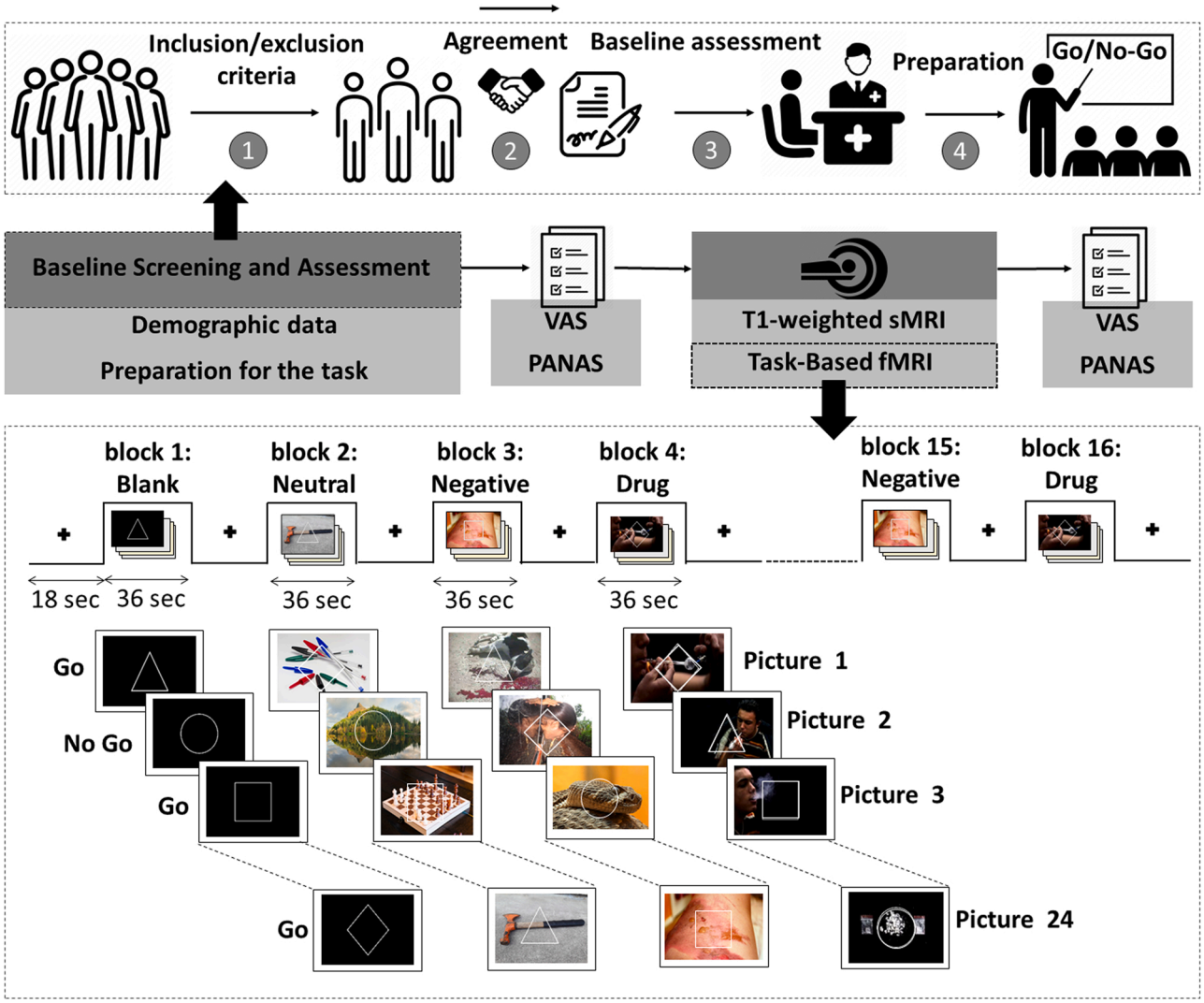

Fig. 1. Summary of the study protocol and the mixed Go/No-Go cue-reactivity task. At the baseline screening and assessment, (1) if subjects passed our inclusion/exclusion criteria, they were invited to the center for further assessment. (2) Subjects were asked to sign the agreement. (3) Subjects were interviewed by a clinical psychologist to collect baseline data. (4) Subjects were trained for the Go/NoGo task and prepared for the scanning session. Immediately before and after scanning PANAS and VAS measures were administered to each subject. During the scanning session, high-resolution T1-weighted and task-based fMRI were collected. The bottom part of the figure shows the Go/NoGo fMRI task design. Each of the four runs of the task included four blocks, adding up to 16 blocks overall. In each block, geometric Go and No-Go stimuli were superimposed on either blank, neutral, emotionally negative, or methamphetamine-related cues. The 'Go' stimuli were polygonal and the 'NoGo' stimulus was a circle. Omission and commission error rates and reaction times were recorded during the task for each individual. In this figure, negative affective and neutral images from the IAPS database are replaced with images from the Wikimedia Commons (full attributations appear in the supplementary materials).

System database and matched for visual complexity (Lang et al., 1997). Participants viewed each cue only once. Go stimuli were triangles, squares, or diamonds and No-Go stimuli were circles. Of the 24 trials in each block, 6 were No-Go and 18 were Go trials. Each stimulus lasted for 1000 ms and was followed by a jittered interstimulus interval (generated using a gamma function, mean = 500 ms). The duration of stimuli and intervals is largely in-line with previous research using simple or mixed Go/No-Go tasks during fMRI scanning (Gilman et al., 2018; Seok and Sohn, 2020; Stein et al., 2021). Blocks were separated by 18-second fixation periods in which a white cross was shown on a black background. Participants were asked to respond as fast as possible when the Go stimuli were presented and withhold their response when seeing No-Go stimuli. Before the scanning session, participants underwent a training test outside the scanner and were informed that both speed and accuracy are important (Fig. 1).

2.4. Scanning Parameters

Scanning was conducted in a 3.0 Tesla (Siemens, MAGNETOM Trio; Germany) MR-system (Neuroimaging and Analysis Group (NIAG); Imam Khomeini Hospital, Tehran, Iran). Structural T1-weighted images were acquired in a sagittal orientation employing a magnetization-prepared rapid gradient-echo (MP-RAGE) sequence with the following parameters: Repetition Time = 1800 ms, Echo Time = 3.44 ms, field of view (FOV) = 256 cm × 256 cm, flip angle (FA) = 7°, 1mm3 Voxels. Functional MRI data were obtained using a gradient-echo echo-planar imaging (GRE-EPI) sequence with the following parameters: FOV = 192 × 192, FA = 90°, in-plane voxel size 3 m. Each run lasted 13 min and 26 s

2.5. Pre-processing

fMRI analysis was performed using the fMRI Expert Analysis Tool (FEAT), part of FMRIB's Software Library version 6.0.3. The pre-processing procedure consisted of: (1) Skull-stripping to remove non-brain tissue from the structural T1-weighted images, using the Brain Extraction Tool (BET) with default values, (2) Removal of first five time points, (3) Motion correction with 6 degrees of freedom (DOF), (4) Interleaved slice-timing correction (5) Spatial smoothing using a Gaussian kernel of FWHM = 5.0 mm, (6) Melodic ICA data exploration to identify remaining data artifacts and to help exploring activation in the data, (7) Multiplicative mean intensity normalization of the volume at each time point, (8) High-pass temporal filtering (Gaussian weighted least-squares straight-line fitting, with Inverse of= 120.0 s),(9) Co-registration of the functional images to the self-high resolution using FMRIB's Linear Image Registration (FLIRT) and Boundary-Based Registration (BBR) cost function, (10) Nonlinear registration of the structural T1 images to the MNI space with 12 degrees of freedom, and (11) Despiking to regress-out the remaining motion effects on fMRI time-series, identified with the DVARS metric given by the FSLMotionOutliers tool. Subjects with a DVARS-threshold> 75 on more than 10 time points in a single block were excluded from the analysis.

2.6. Statistical analysis

Anatomic labeling, and locating the activations were performed using the Brainnetome atlas (BNA)(Fan et al., 2016), with a subsequent visual inspection of different activation clusters, overlaid on the T1-weighted image of the MNI152 atlas. The first-level General Linear Model (GLM) statistical analysis was performed with a Z-threshold of 3.1 and the Cluster Defining Threshold (CDT) method with a corrected p-value< 0.05. In order to calculate the average brain activation for each contrast, higher-level analyses were performed using FMRIB's Local Analysis of Mixed Effects (FLAME) tool (Z-threshold=>3.1, alpha corrected p-value<0.05).

Event-types were specified at the time of indicator onset and the canonical hemodynamic response was used to model the regressors for the conditions of interest. The event types included Blank Successful No-Go (BSNG), Blank Successful Go (BSG), Neutral Successful No-Go (NSNG), Neutral Successful Go (NSG), Negative Successful No-Go (NENG), Negative Successful Go (NESG), Drug Successful No-Go (DSNG), and Drug Successful Go (DSG). Each event type was included as a single regressor. Unsuccessful trials were modeled by a single nuisance regressor in the GLM. Cue-reactivity contrasts were examined as *(Drug>Neutral)* for drug cue-reactivity and (*Negative>Neutral*) for negative emotional cue-reactivity for individuals with MUD and HCs. The response-inhibition contrast was defined as *[(BSNG+NSNG+NESNG+DSNG> BSG+NSG+NESG+DSG)]*. The interaction between cue-reactivity and response-inhibition was modeled with the [*(DSNG>DSG)> (NSNG>NSG)*] contrast for drug and [*(NESNG>NESG)> (NSNG>NSG)*] contrast for negative cues. Six realignment and high-motion parameters based on DVARS metrics were included as nuisance regressors to correct head movement. Finally, a two-sample t-test had been done to compare individuals with MUD and HCs, was calculated.

All behavioral and clinical data were analyzed using R software. Masks and first-level parameter estimates for the activation clusters in each contrast were extracted (R Core Team, 2013), and the correlations of subject parameter estimates and the relevant behavioral and clinical variables, including meth use duration, pre-and post-scanning VAS, pre-and post-scanning negative PANAS, BIS (sum and motor subscale scores), risky behavior history, and commission error rates on the Go/No-Go task. We also compared individuals with MUD with and without drug use in the month before scanning. The significance level was adjusted for multiple comparisons using Bonferroni correction ($\alpha = 0.05$).

3. Results

3.1. Participant characteristics

Demographic and clinical profiles are summarized in Table 1. Significant differences were found between HCs and individuals with MUD in terms of BIS and DASS scores.

3.2. Behavioral performance on the Go/No-Go task

Average commission error rate across participants was 10.91% (SD= 9.00), average omission error rate was 9.59% (SD= 8.17), and average response time was 0.74 s (SD= 0.06). Based on repeated-measures ANOVA test results, commission error rates, omission error rates, and response times differed significantly between blocks (all p-values<0.001). Bonferroni-corrected post-hoc t tests revealed that the percentage of commission errors in neutral (Mean= 11.32, SD= 10.50), negative (Mean= 12.50, SD= 11.29) and drug (Mean= 13.29, SD= 13.89) blocks were significantly higher than in blank blocks (Mean= 6.53, SD= 7.98). The percentage of omission errors in neutral (Mean= 9.93, SD= 10.59), negative (Mean= 12.42, SD= 10.25) and drug (Mean= 12.92, SD= 11.09) cue blocks were also significantly higher than in blank blocks (Mean=3.09, SD=3.79), and the percentage of omission error rates in neutral blocks was significantly lower than in drug cue blocks (p-corrected= 0.017). Average response time in the blank blocks (Mean=674.28, SD=69.61) was significantly faster than in neutral (Mean= 761.37, SD= 60.17), negative (Mean= 768.40, SD= 54.31) and drug (Mean= 757.27, SD= 59.46) blocks, and average response time in drug cue blocks was slightly faster than in negative cue blocks (p-corrected= 0.026) (Fig. 2 and Table S1). Changes in PANAS and VAS scores before and after the cue-reactivity task are presented in Fig. S1.

Table 1
Characteristics of participants (n = 76).

Variables	Individuals with MUD (n = 53)	Healthy Controls (n = 23)
Demographic Variables		
Age (years)	32.12(5.89)	31.17(5.69)
Education (years)	10.08(3.07)	11.91(2.96)
Substance use Patterns		
Total abstinence duration (Day)	81.6(121.5)	–
Total drug abuse duration (months)	146.3(77.3)	–
Hallucinogens		
Number of users	4(7%)	–
Use frequency	2.83(7.5)	–
Opioids		
Number of users	47(88%)	–
Use frequency	22.96(12.6)	–
Cannabis		
Number of users	34(64%)	–
Use frequency	16.5(14.3)	–
Sedatives		
Number of users	12(22%)	–
Use frequency	5.6(10.9)	–
Cocaine		
Number of users	4(7%)	–
Use frequency	2.6(8.1)	–
Alcohol		
Number of users	22(41%)	–
Use frequency	12(13.8)	–
Treatment History		
Treatment in last month	1.98(0.12)	–
Times of treatment in last year	2.67(3.60)	–
NA participation history	1.77(0.42)	–
NA Duration (Months)	15.46(25.42)	–
Clinical Scales		
BIS Scores	75.08(15.11)	57.4(14.87)[a]
DASS Scores	27.53(13.60)	24.4(11.52)[a]
Risky Behaviors		
Number of risky behaviors	2.26(1.11)	
Injection History	10(18%)	
Sexual Intercourse	52(98%)	–
Imprisonment History	24(45%)	–
Drug Selling History	22(41%)	–
Fight History	14(26%)	–

Note: Values are denoted either as mean (SD) or number(percentage). For each substance category, users are defined as individuals who have ever used a substance belonging to that category for at least one month. *"Use frequency"* for each substance category is defined as the number of days any substance belonging to that category had been used, during the last month in which substances of that category were used. For individuals who used more than a single substance from one category, the most frequently used substance is chosen as a stand-in for the frequency of using substances from that category. "*Risky Behaviors*" is a score ranging from one to five, indicating the number of risky behavior domains the participant has engaged in. These include "*having ever had illicit sexual intercourse*", "*having ever been imprisoned*", "*having ever injected drugs*", "*having ever sold drugs*", and "*having gotten into any fights in the last month*". Abbreviations: BIS, Barratt Impulsiveness Scale; DASS, Depression Anxiety Stress Scale; VAS, Visual Analog Scale.

[a] Data for these cells exist only for 5 Healthy controls.

3.3. Drug and negative cue-reactivity

In individuals with MUD, drug cue exposure was associated with higher activity compared to neutral cue exposure in the left lateral superior frontal gyrus (SFG) (4263 voxels, z-max= 6.7), left rostroventral inferior temporal gyrus (ITG) (1179 voxels, z-max=6.1), left dorsal (955 voxels, z-max= 7.14), caudodorsal (297 voxels, z-max= 5.16) and pregenual cingulate gyrus (CG) (221 voxels, z-max= 4.86), left ventral caudate basal ganglia (BG) (758 voxels, z-max= 5.14), left caudal inferior parietal lobule (IPL) (409 voxels, z-max= 5.34) and rostroventral IPL (357 voxels, z-max= 4.7), left inferior frontal sulcus (IFS) (406 voxels, z-max= 6.14), right lateral occipital cortex (LOcC) (375 voxels, z-max= 5.47), left orbital gyrus (ORG) (312 voxels, z-max=5.06), caudal ventrolateral precentral gyrus (PrG) (177 voxels, z-max= 4.8), and lower activity compared to neutral cue exposure in the right caudal cuneus (12,600 voxels, z-max= 7.76), left superior temporal gyri (STG) (planum STG (500 voxels, z-max= 5.04), anterior STG (137 voxels, z-max= 4.08), and paracentral lobule (PCL) (110 voxels, z-max= 4.91) corrected p-value< 0.05 (Fig. 3.a and Table S2).

To test the validation of the task, we compared brain activations of drug cue-reactivity (*Drug>Neutral*) contrast between individuals with MUD and HCs. Individuals with MUD had a higher drug cue-reactivity than HCs in the left medial orbital gyrus (323 voxels, z-max=4.19), left inferior frontal junction (307 voxels, z-max=4.64), left lateroventral fusiform gyrus (179 voxels, z-max=4.12) and the right lateral occipital cortex (160 voxels, z-max=4.09), corrected p-value< 0.05 (Fig. 3.b and 3.c and Table S3).

Negative versus neutral cues were associated with higher activations in the cuneus (16,159 voxels, z-max= 8.92), bilateral ORG (left: 229 voxels, z-max= 4.85), (right: 291 voxels, z-max= 5.67) left Inferior Frontal Gyrus (IFG) (259 voxels, z-max= 4.42), bilateral medial amygdala (left:163 voxels, z-max= 5.67), (right= 189 voxels, z-max= 6.23), left occipital thalamus (185 voxels, z-max= 4.56), and left lateral SFG (182 voxels, z-max= 5.36), and lower activations in the left postcentral gyrus (POG) (5059 voxels, z-max= 5.69), right caudal IPL (2931 voxels, z-max= 6.11), ventromedial middle frontal gyrus (MFG) (2105 voxels, z-max= 5.04), and bilateral intermediate lateral ITG (left: 318 voxels, z-max=5.08, right: 1032 voxels, z-max= 5.45), dorsal CG (907 voxels, z-max= 5.24), Operculum IFG (635 voxels, z-max= 4.99), with a corrected p-value< 0.05 (Fig. 4, and Table S4).

3.4. Response-inhibition

In the overall No-Go>Go response-inhibition contrast (*DSNG+NSNG+BSNG+NESNG*) >(*DSG+NSG+BSG+NESG*), activations survived a corrected p-value< 0.05 threshold in the left rostroventral IPL (1522 voxels, z-max=5.64), right anterior superior MTG (1515 voxels, z-max= 5.36), left medial precuneus (Pcun) (777 voxels, z-max= 4.57), left lateral SFG (169 voxels, z-max= 4.34), right rostral IFG (124 voxels, z-max= 4.38) and right pregenual CG (116 voxels, z-max= 4.09). Go trials were associated with higher activations than No-Go trials in the right medioventral FUG (3305 voxels, z-max= 6.7), Left POG (2632 voxels, z-max= 6.87), and Left caudal cuneus (624 voxels, z-max= 5.97), right medial SFG (381 voxels, z-max= 5.48), left Caudal ventrolateral PrG (346 voxels, z-max= 4.9), left Ventral Caudate (322 voxels, z-max= 4.6), left Medioventral Fusiform Gyrus FuG (297 voxels, z-max= 4.95), left Inferior DLPFC (95 voxels, z-max= 3.67), (Fig. 5, and Table S5).

3.5. Response-inhibition during drug cue-reactivity and negative emotional cue-reactivity

The drug cue-reactivity/response-inhibition interaction contrast revealed a higher activation during drug-related inhibition than neutral cue inhibition in the left caudal cuneus (5129 voxels, z-max= 6.94), right dorsomedial parietooccipital Pcun (137 voxels, z-max=4.28), right medial superior occipital gyrus (116 voxels, z-max= 4.05) and left LOcC (98 voxels, z-max= 3.67), and with lower activation in the bilateral POG (left: 1647 voxels, z-max= 4.49, right: 319 voxels, z-max= 4.54), right caudodorsal CG (1317 voxels, z-max= 4.61), right rostroventral IPL (776 voxels, z-max= 4.36), left medial SFG (352 voxels, z-max= 4.15), and right dorsal agranular insula (152 voxels, z-max= 4.32), corrected p-value< 0.05 (Fig. 6, and Table S6).

Response-inhibition during negative cue exposure is associated with greater activity compared to neutral inhibition in the right dorsolateral MTG (369 voxels, z-max= 4.27), and left rostroventral IPL (125 voxels, z-max= 4.11), and lower activity only in the left Lateroventral Fusiform

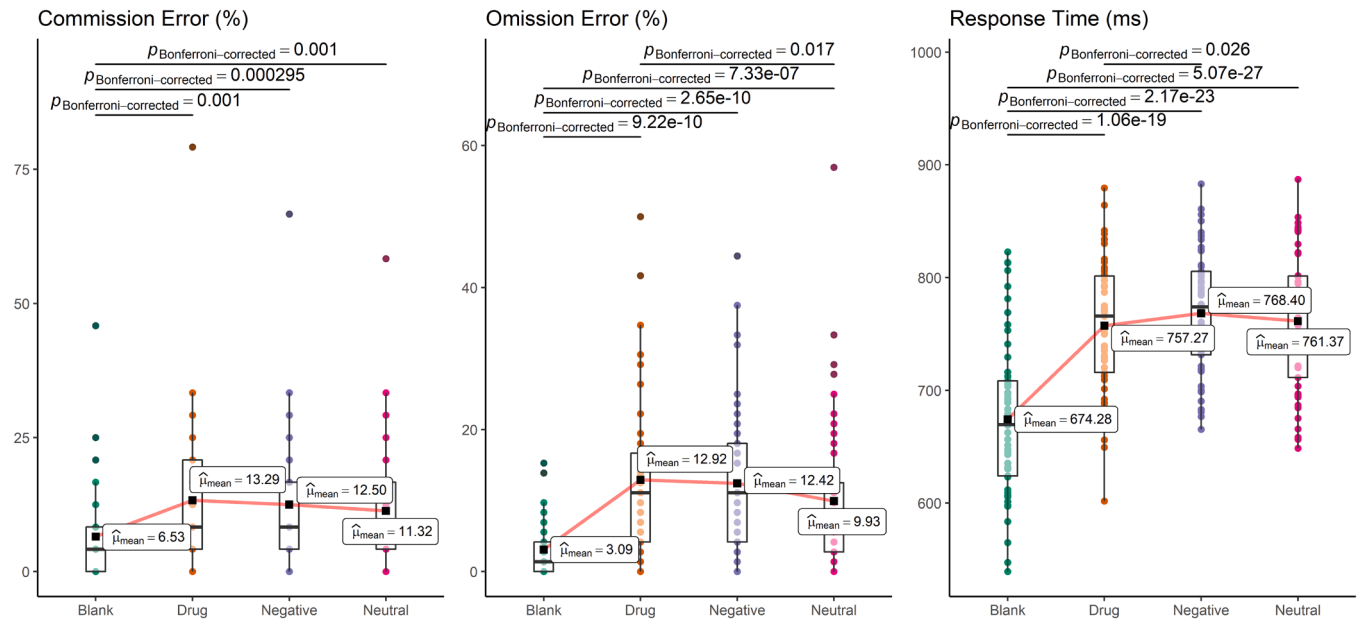

Fig. 2. Behavioral performance. Box and whisker plots showing the behavioral performance of participants with MUD on the Go/No-Go task across the four different block types. ANOVA tests indicated significant differences in error rates and reaction times, and thus post-hoc comparisons were conducted using repeated-measures t tests. Bonferroni-corrected *P*-values are shown for significant pair-wise comparisons between block types. Omission error is defined as failing to respond to Go trials, and commission error is the failure to inhibit pre-potent responses on No-Go trials.

Gyrus (277 voxels, z-max= 4.43), corrected p-value< 0.05 (Fig. 7 and Table S7).

3.6. Correlates of brain activation

The negative interaction contrast in the right dorsolateral MTG cluster (beta= −0.357, p-corrected= 0.018) had Bonferroni-corrected significant correlations with the pre-scanning negative PANAS and BIS motor inhibition scores (beta= −0.319, p-corrected= 0.04). Several other correlations between the cue-reactivity, response-inhibition and interaction contrasts and behavioral variables were significant based on uncorrected p-values, but were not significant after Bonferroni correction for multiple comparisons (Table S8).

4. Discussion

This study adds to the scant literature on the interaction of response-inhibition and reactivity to negative and drug cues, developing the first mixed fMRI response-inhibition task which can assess response-inhibition in the presence of negative and drug cue-reactivity in individuals with methamphetamine use disorder (MUD). Subsequently, we validated this task by demonstrating behavioral and neural evidence of the influence of negative and drug cue presentation on response-inhibition. The implications of the observed brain activations and deactivations will be discussed below, along with their correlations with subjective craving and markers of inhibitory performance.

Affectively-driven impulsivity has been shown to involve activity in several brain regions relevant in both emotion regulation and cognitive control, such as the anterior insula and the orbitofrontal cortex (Johnson et al., 2020). These neural correlates are shared with addictive disorders (Um et al., 2019), and potentially implicate top-down inhibitory impairments when processing salient stimuli (Heatherton and Wagner, 2011).

4.1. Cue-reactivity

Drug cue-reactivity was associated with activations in the striatum, the superior frontal and pregenual anterior cingulate gyri (CG), IFG, and limbic regions, cuneus and amygdala. Our findings are in line with previous methamphetamine cue-reactivity studies showing that these regions are more activated than healthy controls when comparing brain reactivity to methamphetamine cues to other cues (Grodin et al., 2019; Yin et al., 2012). While the striatum and anterior CG are important nodes in the reward network (Luijten et al., 2017; Zilverstand et al., 2018), the SFG is broadly implicated in decision making (Boisgueheneuc et al., 2006). The observed SFG activation may be related to reward-related decision making during drug cue-reactivity, as SFG activity is influenced by dopaminergic pathways during reward appraisal (Ott and Nieder, 2019) and has been observed in SUDs (Garavan et al., 2000; Grüsser et al., 2004). The IPL and dorsal CG had increased activations during drug cue-reactivity but decreased activity in negative emotional cue-reactivity. As nodes of the salience network (Zilverstand et al., 2018), the IPL and dorsal CG are involved in drug craving and drug-seeking (Kühn and Gallinat, 2011; Naqvi and Bechara, 2009), and the different effects of drug cue-reactivity and negative emotional cue-reactivity on their activity may indicate the redirecting of attentional resources towards drug cues and away from negative cues (Corbetta et al., 2008; Shenhav et al., 2013). On the other hand, the IFG was activated in both drug cue-reactivity and negative emotional cue-reactivity. The IFG's involvement in drug cue-reactivity has been reported before (Hanlon et al., 2018; Reuter et al., 2005), but it also plays a vital role in processing conflicts between opposing representations and may have been engaged by our complicated task design to resolve the resulting conflicts (Novick et al., 2005; Swick et al., 2008). Notably, individuals with MUD also differed from HCs in the drug cue-reactivity-associated activation of the inferior frontal junction, which borders the IFG.

Lastly, we also observed altered drug cue-reactivity and negative cue-reactivity-associated activations in the cuneus, which is part of the default mode network (DMN) and is involved in episodic memory retrieval (Xu et al., 2016), and the amygdala, central to the processing of salient stimuli as part of the limbic network (Chase et al., 2011; Dickerson and Eichenbaum, 2010; Tang et al., 2012). Increased functional activity in the posterior part of the DMN, together with decreased MFG activation, suggests the engagement of self-referential processing during negative emotional cue-reactivity (Xu et al., 2016). Increased amygdalar

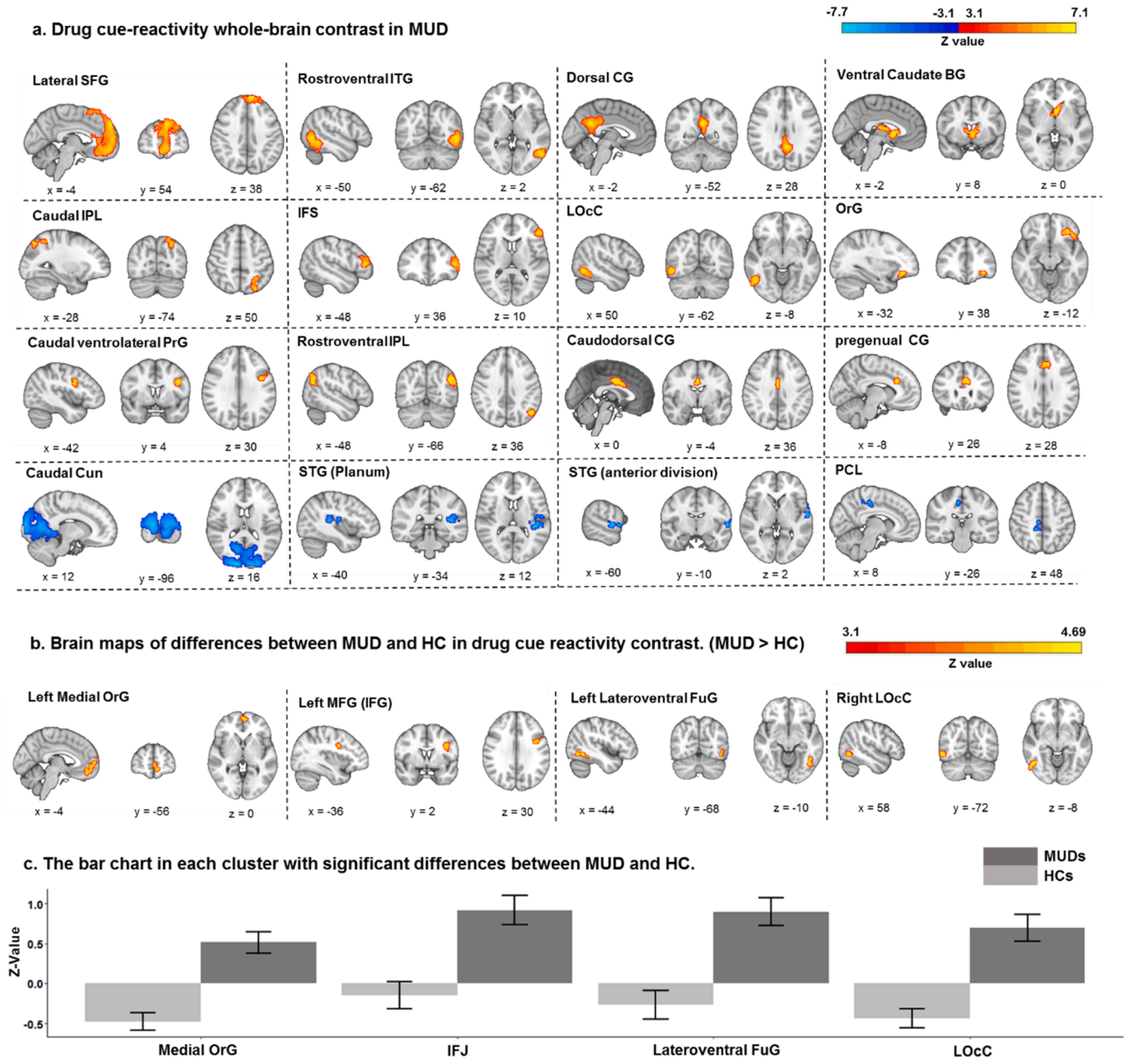

Fig. 3. Drug cue-reactivity. a. Significant clusters in the drug cue-reactivity whole-brain contrast in individuals with MUD surviving the FDR-corrected $p < 0.05$ threshold. Positive z-values (in warm colors) indicate higher voxel activations associated with methamphetamine compared to neutral cues, while negative z-values (in cold colors), indicate the reverse. MNI coordinate of the voxel with the maximal z-value in each cluster is reported bellow sagittal, coronal, and axial views. 16 significant clusters are visualized based on the cluster-defining threshold method and reported based on the Brainnetome atlas parcellation: left lateral superior frontal gyrus (Lateral SFG, 4263 voxels), left rostroventral inferior temporal gyrus (Rostroventral ITG, 1179 voxels), left dorsal cingulate gyrus (Dorsal CG, 995 voxels), left ventral caudate basal ganglia (Ventral Caudate BG, 758 voxels), left caudal inferior parietal lobule (Caudal IPL, 409 voxels), left rostroventral inferior parietal lobule (Rostroventral IPL, 357 voxels), left inferior frontal sulcus (IFS, 406 voxels), right lateral occipital cortex (LOoC, 375 voxels), left orbital gyrus (OrG, 312 voxels), left caudodorsal cingulate gyrus (Caudodorsal CG, 27 voxels), left pregenual cingulate gyrus (Pregenual CG, 221 voxels), left caudal ventrolateral precentral gyrus (Caudal ventrolateral PrG, 177 voxels), caudal cuneus (Caudal Cun, 12,600 voxels), left superior temporal gyrus (Planum) (STG(Planum), 500 voxels), left superior temporal gyrus (anterior division) (STG (anterior division), 137 voxels), paracentral lobule (PCL, 110 voxels). b. Clusters with significant between-group differences in the drug cue-reactivity contrast between individuals with MUD and HCs. All clusters survived the FDR-corrected $p < 0.05$ threshold, and have higher drug>neutral activations in individuals with MUD compared to HCs (indicated by warm colors). Four significant clusters were found: Medial orbital gyrus (Medial OrG, 323 voxels), left inferior frontal junction (IFJ, 307 voxels), left lateroventral fusiform gyrus (Lateroventral FuG, 179 voxels), right lateral occipital cortex (LOcC, 160 voxels) c. The bar chart in the clusters with significant differences between individuals with MUD and HCs in drug cue-reactivity contrast. The bars estimate the mean z-value in the drug cue-reactivity contrast in each cluster. The error bars show the standard error of z-statistic values across 53 individuals with MUD and 23 HCs. HCs: healthy controls, MUD, methamphetamine use disorder.

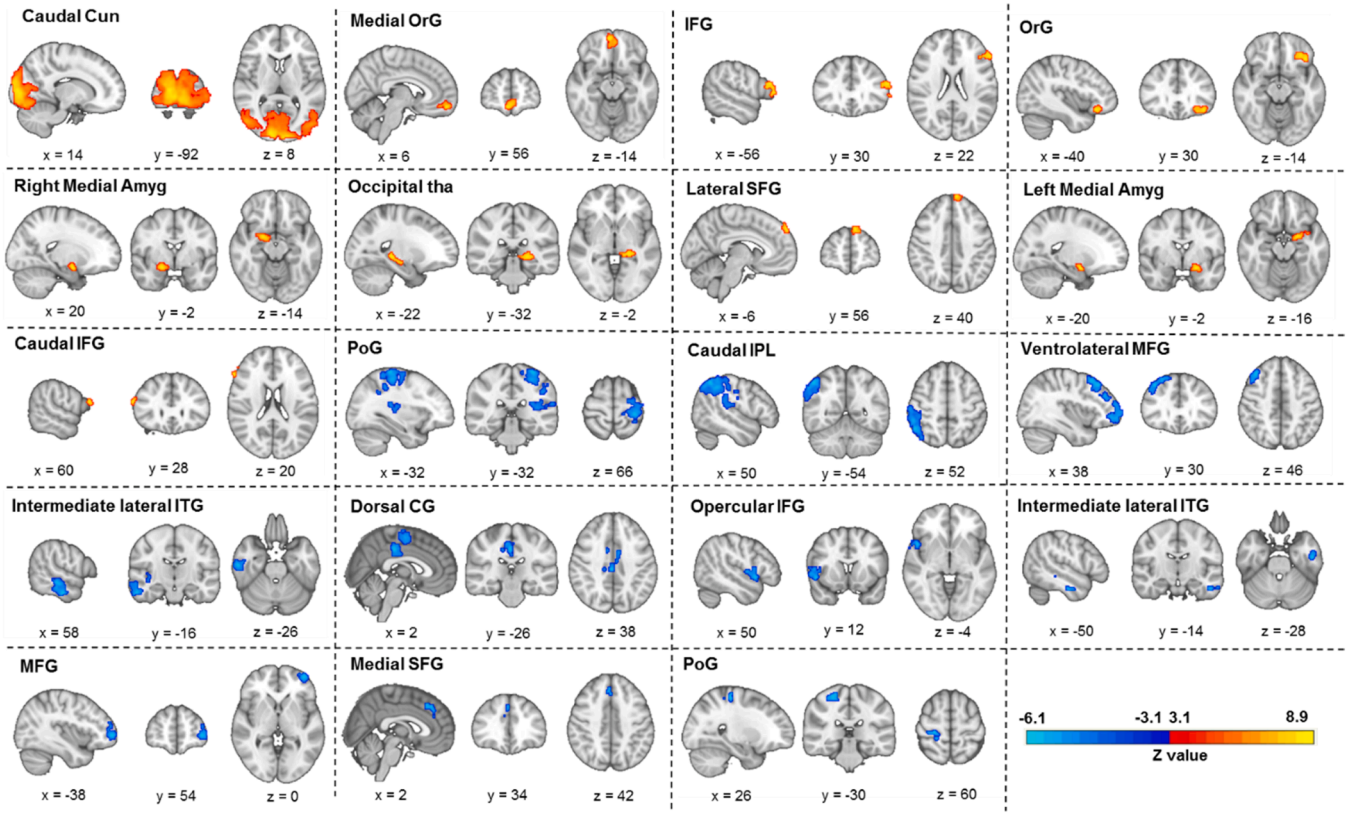

Fig. 4. Negative cue-reactivity. Significant clusters in the negative cue-reactivity whole-brain contrast in individuals with MUD surviving the FDR-corrected $p < 0.05$ threshold. Voxels with positive z-values are displayed with warm colors (red to yellow) and show a higher activation associated with negative compared to neutral cues, while voxels with negative z-values are displayed with cold colors (blue to cyan) and have a higher activation when viewing neutral compared to negative cues. MNI coordinate of the peak voxel in each significant cluster is reported bellow sagittal, coronal, and axial views of the brain. 19 significant clusters are visualized based on cluster-defining threshold method and reported based on Brainnetome atlas parcellation as follow: caudal cuneus (Caudal Cun, 16,159 voxels), medial orbital gyrus (Medial OrG, 291 voxels), left inferior frontal gyrus (IFG, 259 voxels), left orbital gyrus (OrG, 229 voxels), medial amygdala (Right Medial Amyg, 189 voxels, Left Medial Amyg, 163 voxels), left occipital thalamus (Occipital tha, 185 voxels), left lateral superior frontal gyrus (Lateral SFG, 182 voxels), right caudal inferior frontal gyrus (Caudal IFG, 128 voxels), left postcentral gyrus (PoG, 5059 voxels), right caudal inferior parietal lobule (Caudal IPL, 2931 voxels), right ventrolateral middle frontal gyrus (Ventrolateral MFG, 2105 voxels), intermediate lateral inferior temporal gyrus (Right Intermediate lateral ITG, 1032 voxels, left Intermediate lateral ITG, 318 voxels), Dorsal Cingulate Gyrus (Dorsal CG, 907 voxels), right Operculum (Opercular IFG, 635 voxels), left middle frontal gyrus (MFG, 195 voxels), right medial superior frontal gyrus (Medial SFG, 157 voxels), right postcentral gyrus (PoG, 156 voxels).

and cuneal activation in response to negative versus neutral cues was also observed in HCs, suggesting that negative emotional cue-reactivity can generally engage emotional and self-referential processing in all participants.

4.2. Response-inhibition

Response-inhibition was associated with activations in the left IPL and SFG, and right insula, MTG, IFG and the anterior cingulate cortex. All these regions are known to be involved in successful response-inhibition, supporting the validity of the task and the chosen contrast (Aron, 2007; Dong et al., 2012; Duann et al., 2009; Gruber and Yurgelun-Todd, 2005; Hampshire et al., 2010; Mostofsky and Simmonds, 2008; Tapert et al., 2007). Notably, the right-lateralization of IFG and IPL, import nodes in the inhibitory frontoparietal network, has been observed in previous research on response-inhibition as well (Garavan et al., 1999, 2002; Hampshire et al., 2010; McNab et al., 2008). We also observed occipital and precuneal activations which, while more rarely observed, have been reported in some previous studies (Braver et al., 2001; Kelly et al., 2004; Liddle et al., 2001; Mathalon et al., 2003; Wager et al., 2005). Despite these similarities, caution should be exercised when comparing the neural substrates of response-inhibition across studies, as the fMRI activation patterns associated with response-inhibition are task-dependent (Swick et al., 2011; Yeung et al., 2020), and different response-inhibition tasks may variably engage associated processes such as response selection (Simmonds et al., 2008). For example, while most of the cited research suggests a hyperactivation of inhibitory regions in SUDs, it has been noted that some studies suggest reverse alterations of response-inhibition-associated neural activity (Zilverstand et al., 2018).

4.3. Interaction of response-inhibition, drug cue-reactivity and negative emotional cue-reactivity

Higher commission and omission error rates and longer reaction times in drug and negative cue blocks compared to blank blocks may indicate an impairing influence of drug cue-reactivity and negative emotional cue-reactivity on response-inhibition, and such inhibitory impairments have been observed frequently on studies of response-inhibition during exposure to drug (Czapla et al., 2015; Lannoy et al., 2019; Noël et al., 2007; Weafer and Fillmore, 2012) or emotionally negative cues (Albert et al., 2010; Goldstein et al., 2007; Ramos-Loyo et al., 2017). Notably however, only drug blocks were associated with higher error compared to neutral blocks, suggesting that much of the behavioral impact on task performance may be due to the added requirement for visual processing. But the neural patterns associated with general response-inhibition diverge markedly from those involved in response-inhibition during drug or negative cue-reactivity, pointing

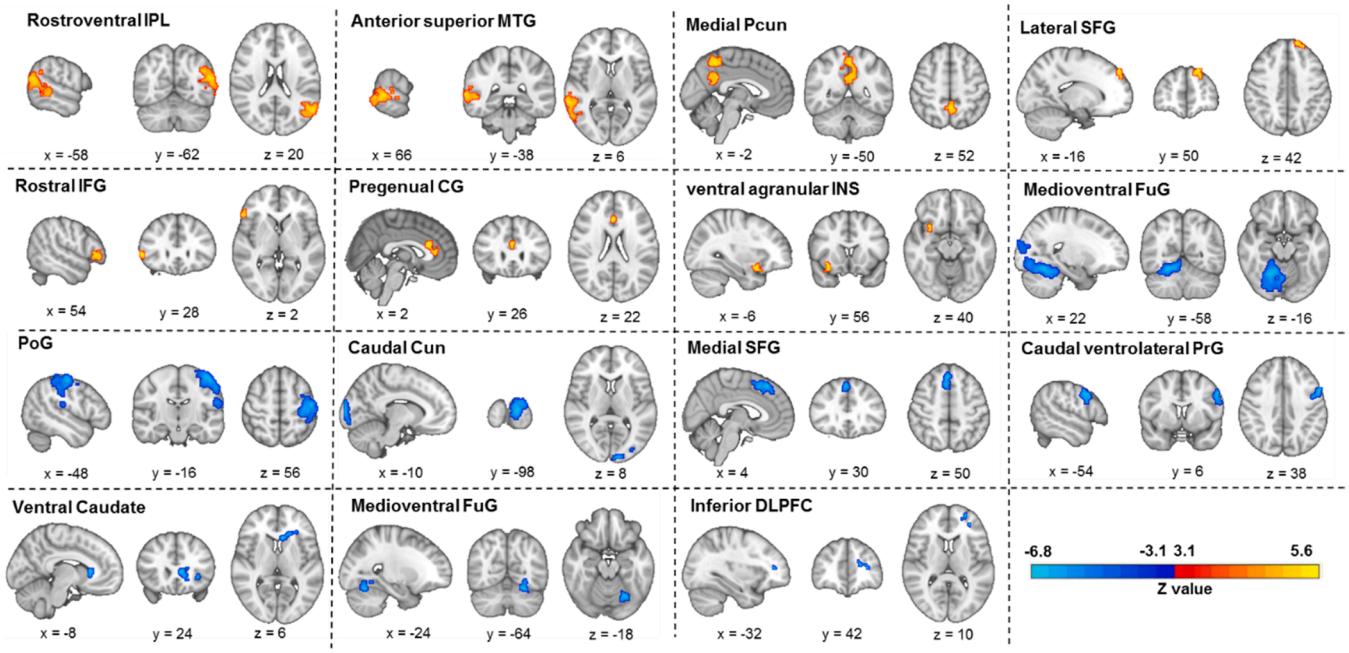

Fig. 5. Response-inhibition. Significant clusters in the response-inhibition whole-brain contrast in individuals with MUD surviving the FDR-corrected $p < 0.05$ threshold. Voxels with positive z-values are displayed with warm colors (red to yellow) and show a higher activation associated with No-Go compared to Go trials, while voxels with negative z-values are displayed with cold colors (blue to cyan) and have a higher activation during Go compared to No-Go trials. MNI coordinate of the peak voxel in each significant cluster is reported bellow sagittal, coronal, and axial views of the brain. 15 significant clusters are visualized based on cluster-defining threshold method and reported based on Brainnetome atlas parcellation as follow: left rostroventral inferior parietal lobule (Rostroventral IPL, 1552 voxels), right anterior superior middle temporal gyrus (Anterior superior MTG, 1515 voxels), middle precuneus (Middle Pcun, 777 voxels), left lateral superior frontal gyrus (Lateral SFG, 169 voxels), right rostral inferior frontal gyrus (Rostral IFG, 124), pregenual cingulate gyrus (Pregenual CG, 116 voxels), right ventral agranular insular gyrus (Ventral agranular INS, 71 voxels), right medioventral fusiform gyrus (Medioventral FuG, 3305 voxels), left postcentral gyrus (PoG, 2632 voxels), left caudal cuneus (Caudal Cun, 624 voxels), medial superior frontal gurus (Medial SFG, 381 voxels), left caudal ventrolateral precentral gyrus (Caudal ventrolateral PrG, 346 voxels), left ventral caudate (Ventral Caudate, 322 voxels), left medioventral fusiform gyrus (Medioventral FuG, 297 voxels), left inferior dorsolateral prefrontal cortex (inferior DLPFC, 95 voxels).

to the engagement of different processes in either case. Response-inhibition during drug cue-reactivity was associated with higher activations in the bilateral visual cortices and cunei and lower activations in regions associated with response-inhibition (MFG and IPL), motor control (precentral gyrus, supplementary motor area) and interoception (insula). Interestingly, the bilateral caudal cuneus and superior occipital lobe were deactivated during neutral response inhibition, demonstrating that drug cues might directly impair response-inhibitory processes. This poorer recruitment of inhibitory control resources during cue-reactivity has been observed before (Batterink et al., 2010; Gilman et al., 2018; Liu et al., 2014; Seok and Sohn, 2020) and might reflect a shifting of neural resources to processing addiction-relevant cues, due to their high salience (Czapla et al., 2017; Stein et al., 2021). A disinhibited neural state may also come about due to the conflict between response-inhibition and approach bias to drug cues (Kreusch et al., 2013).

Response-inhibition was associated with a higher activation when viewing negative compared to neutral cues in the right MTG and left IPL, and a lower activation in the left fusiform gyrus. Strikingly, these regions mostly have the exact same pattern of activity during general response inhibition: Superior temporal and IPL regions are activated for response-inhibition, while the fusiform gyrus is deactivated. This pattern potentially indicates increased neural inhibitory effort aimed at maintaining appropriate inhibitory control. While it's unclear why these and not other regions would show this compensatory activity pattern, there is evidence that activity patterns in the MTG and IPL, especially the supramarginal gyrus, are associated with response-inhibition impairments in individuals with addictive disorders during conventional Go/No-Go tasks (Chikazoe et al., 2007; Qiu and Wang, 2021) and response-inhibition when viewing negative cues (Brown et al., 2012; Chester et al., 2016; Goldstein et al., 2007). Right MTG activation was also significantly correlated with pre-scanning negative affect and self-reported motor impulsivity, indicating that the MTG may be an essential hub for the interaction of negative affective processing and response-inhibition. More investigations of the role of IPL and MTG activity in negative urgency in MUD are warranted given the broader involvement of these regions in the neurobiology of the disorder (Jan et al., 2012; Paulus and Stewart, 2020; Sabrini et al., 2019). Taken together, our study is the first to show that a mixed Go/No-Go task can reveal notable differences in the neural substrates of general response-inhibition and response-inhibition during drug and negative cue-reactivity, especially in the IPL, MTG, and occipital regions. Our exploratory analyses also suggest that disinhibition during drug cue-reactivity and dysfunctional compensatory over-activation during negative cue-reactivity may be involved in positive and negative urgency. A general view of the neuro-cognitive model that informs and is supported by this study is provided in Fig. 8.

4.4. Limitations

This project has a number of notable limitations. In terms of participants, the sample size is substantial but includes no female subjects, and while data from HCs was used only to validate the reactivity of MUD participants to methamphetamine cues, sample sizes were unbalanced. The MUD participants were also heterogeneous in certain respects, and the methamphetamine use duration had a high variance. Regarding the task design, factorial and mixed tasks limit the statistical power of inference on different conditions of interest. Lastly, the inherently cross-sectional nature of this study precludes a prospective investigation of correlations between neural activity and clinically-relevant outcomes

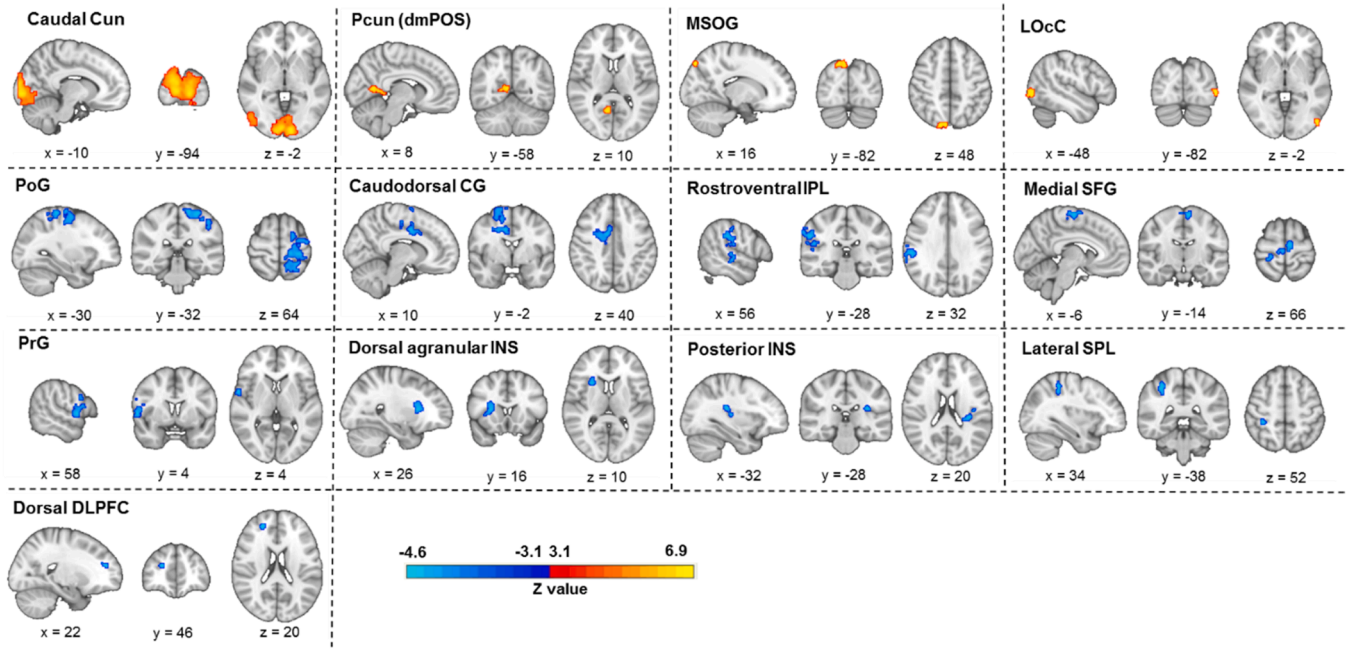

Fig. 6. Drug cue-reactivity/ response-inhibition interaction. Significant clusters in the drug cue-reactivity/response-inhibition interaction whole-brain contrast in individuals with MUD surviving the FDR-corrected $p < 0.05$ threshold. Voxels with positive z-values are displayed with warm colors (red to yellow) and show a higher activation associated with response-inhibition during exposure to methamphetamine compared to neutral cues, while voxels with negative z-values are displayed with cold colors (blue to cyan) and have a higher activation during response-inhibition when viewing neutral compared to methamphetamine cues. MNI coordinate of the peak voxel in each significant cluster is reported bellow sagittal, coronal, and axial views of the brain. 13 significant clusters are visualized based on cluster-defining threshold method and reported based on Brainnetome atlas parcellation as follow: caudal cuneus (Caudal Cun, 5129 voxels), right dorsomedial parietooccipital precuneus (Pcun (dmPOS), 137 voxels), right medial superior occipital gyrus (MSOG, 116 voxels), left lateral occipital cortex (LOcC, 98 voxels), left postcentral gyrus (PoG, 1647 voxels), right caudodorsal cingulate gyrus (Caudodorsal CG, 1317 voxels), right rostroventral inferior parietal lobule (Rostroventral IPL, 776 voxels), medial superior frontal gyrus (Medial SFG, 352 voxels), right precentral gyrus (PrG, 319 voxels), right dorsal agranular insula (Dorsal agranular INS, 152 voxels), left posterior insular gyrus (Posterior INS, 124 voxels), left lateral superior parietal lobule (Lateral SPL, 84 voxels), left dorsal dorsolateral prefrontal cortex (Dorsal DPLFC, 69 voxels).

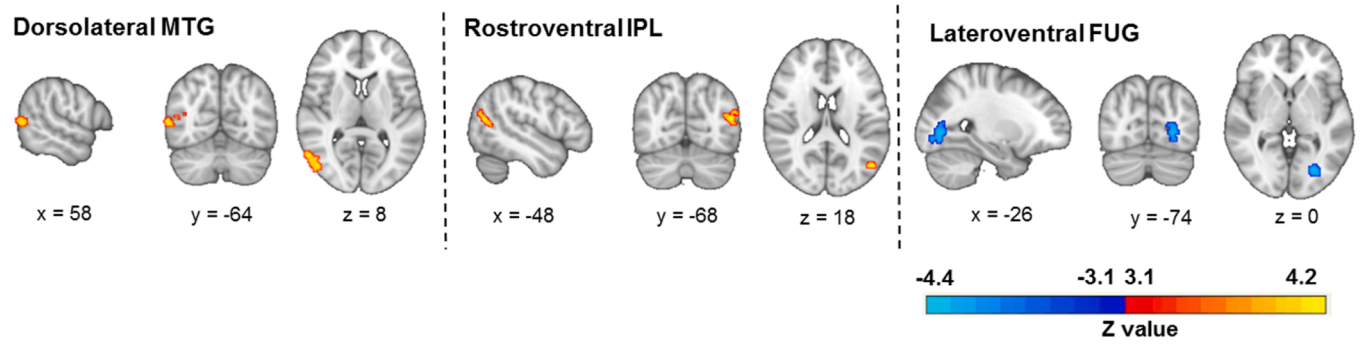

Fig. 7. Negative cue-reactivity/ response-inhibition interaction. Significant clusters in the negative cue-reactivity/response-inhibition interaction whole-brain contrast in individuals with MUD surviving the FDR-corrected $p < 0.05$ threshold. Voxels with positive z-values are displayed with warm colors (red to yellow) and show a higher activation associated with response-inhibition during exposure to negative compared to neutral cues, while voxels with negative z-values are displayed with cold colors (blue to cyan) and have a higher activation during response-inhibition when viewing neutral compared to negative cues. MNI coordinate of the peak voxel in each significant cluster is reported bellow sagittal, coronal, and axial views of the brain. 3 significant clusters are visualized based on cluster-defining threshold method and reported based on Brainnetome atlas parcellation as follow: right dorsolateral middle temporal gyrus (Dorsolateral MTG, 369 voxels), left rostroventral inferior parietal lobule (Rostroventral IPL, 125 voxels) and left lateroventral fusiform gyrus (Lateroventral FUG, 277 voxels).

such as relapse or treatment response over time, which will be important in future research using this task.

4.5. Conclusion

Besides adding to the literature on the neural substrates of response-inhibition and reactivity to emotionally negative and drug-associated cues in MUD, this is the first study on the fMRI-correlates of the interactions of these phenomena in this addictive disorder. There is already some evidence that drug cue-reactivity and response-inhibition fMRI paradigms may help develop biomarkers to aid diagnosis, prognosis, and treatment monitoring (Bough et al., 2014; Garrison and Potenza, 2014; Zilverstand et al., 2018). Studies using mixed response-inhibition tasks may further aid translational efforts (Noël et al., 2007), and recent research suggests that response-inhibition during cue-reactivity can elicit neural activations that predict clinically relevant outcomes such as relapse (Gilman et al., 2018). Considering the engagement of various regions known to be involved in the

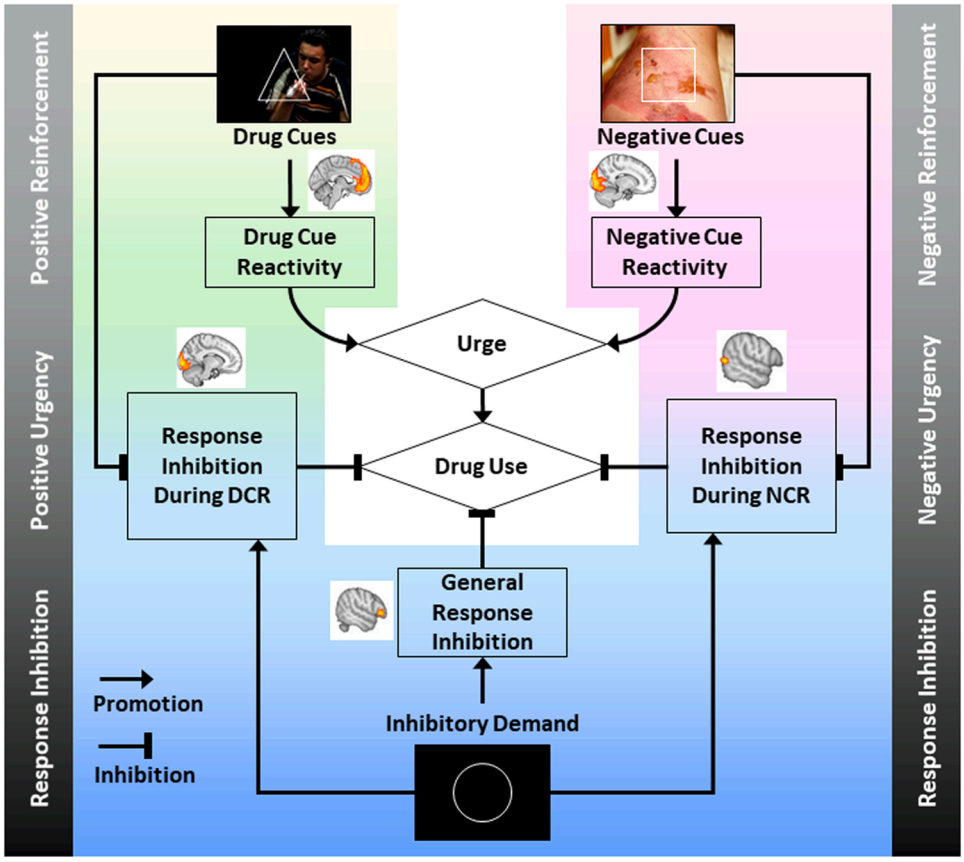

Fig. 8. Interaction of response inhibition and cue-reactivity. Exposures to drug and negative cues can induce methamphetamine use urges and culminate in drug use, whereas response inhibitory processes can inhibit such behavior. However, response-inhibitory processes are rarely engaged in isolation in individuals with methamphetamine use disorder. Often, response-inhibition occurs in the presence of drug and negative cues, which interact with and modulate response-inhibitory processes during experiences of urgency. Some of the neural correlates of different isolated and interacting processes are highlighted. Cues used in the image are taken from the mixed task. Geometric No-Go (circle) and Go (other shapes) stimuli are superimposed over blank, neutral, negative emotional, or methamphetamine-related images. In this figure, the negative affective image from the IAPS database on the top-right is replaced with an image from the Wikimedia Commons (full attributation appears in the supplementary materials).

neurobiology of SUDs by our mixed Go/No-Go task and the modulation of response-inhibitory activity by cue-induced craving and negative affect, further consideration of these paradigms is warranted. Future research should use longitudinal designs and multicentric scanning to assess the reliability and generalizability of various activation patterns, and measure clinical outcomes and their co-variation with these patterns to elucidate their precise role in the MUD, potentially aiding the discovery of novel targets for intervention (Paulus and Stewart, 2020) or clinical course prediction (Gilman et al., 2018).

Role of Funding Source

Tehran University of Medical Sciences approved and provided the funding for this study under the code 93–02–98–23869. This funding source had no role in the design of this study and will not have any role during its execution, analyses, interpretation of the data, or decision to submit results.

Funding

This work was supported by the Tehran University of Medical Sciences (Tehran, Iran) and also partially by the Cognitive Sciences and Technologies Council (Tehran, Iran) under the grant numbers 9336 and 8651.

CRediT authorship contribution statement

Amirhossein Dakhili: Writing – original draft, Methodology, Formal Analysis, Data Collection, **Arshiya, Sangchooli**: Writing – original draft, Methodology, Writing – review & editing, Visualization, **Sara Jafakesh**: Writing – original draft, Methodology, Visualization, Software, **Mehran Zare-Bidoky**: Writing – original draft, Investigation, **Ghazaleh Soleimani**: Writing – original draft, Writing – review & editing, **Seyed Amir Hossein Batouli**: Data collection, Conceptualization, Software, **Kamran Kazemi**: Investigation, Supervision, **Ashkan Faghiri**: Data collection, Resources, **Mohammad Ali Oghabian**: Data collection, Conceptualization, Resources, **Hamed Ekhtiari:** Supervision, Writing – review & editing, Conceptualization.

Contributors

All Authors have contributed significantly to the work.

A.D., A.S., S.J., M.Z.B, G.S., have contributed in writing the original draft. A.D., A.S, S.J., designed the methodology. A.D., implemented the formal analysis. A.D., M.A.O., S.A.H.B., A.F., contributed in data collection. A.S., G.S., H.E., contributed in writing the final draft. S.J., S. A.H.B., contributed to programming. S.J., A.S., prepared the visualizations. M.Z.B, K.K., were involved in the investigation process. M.A.O., H. E., S.A.H.B., formulated overarching research goals and aims. H.E., K.K., had oversight and leadership responsibilities, and designed the research protocol. M.A.O., A.F., provided necessary materials and resources for the research.

Conflict of Interest

The authors declare that they have no conflict of interest to disclose.

Appendix A. Supporting information

Supplementary data associated with this article can be found in the online version at doi:10.1016/j.drugalcdep.2022.109353.

References

Alam Mehrjerdi, Z., Mokri, A., Ekhtiari, H., 2011. Human laboratory settings for assessing drug craving implications for the evaluation of treatment efficacy. Basic Clin. Neurosci. 2 (3), 5–11.

Albert, J., López-Martín, S., Carretié, L., 2010. Emotional context modulates response inhibition: neural and behavioral data. Neuroimage 49 (1), 914–921.

American Psychiatric Association, 2013. Diagnostic and Statistical Manual of Mental Disorders (DSM-5®). American Psychiatric Pub,.

Ames, S.L., Wong, S.W., Bechara, A., Cappelli, C., Dust, M., Grenard, J.L., Stacy, A.W., 2014. Neural correlates of a Go/NoGo task with alcohol stimuli in light and heavy young drinkers. Behav. Brain Res. 274, 382–389.

Aron, A.R., 2007. The neural basis of inhibition in cognitive control. Neuroscientist 13 (3), 214–228.

Barratt, E., 1994. Impulsivity and aggression In J. Monahan & HJ Steadman. Violence and mental disorder: Developments in risk assessment.

Batterink, L., Yokum, S., Stice, E., 2010. Body mass correlates inversely with inhibitory control in response to food among adolescent girls: an fMRI study. Neuroimage 52 (4), 1696–1703.

Boisgueheneuc, Fd, Levy, R., Volle, E., Seassau, M., Duffau, H., Kinkingnehun, S., Samson, Y., Zhang, S., Dubois, B., 2006. Functions of the left superior frontal gyrus in humans: a lesion study. Brain 129 (12), 3315–3328.

Bough, K.J., Amur, S., Lao, G., Hemby, S.E., Tannu, N.S., Kampman, K.M., Schmitz, J.M., Martinez, D., Merchant, K.M., Green, C., 2014. Biomarkers for the development of new medications for cocaine dependence. Neuropsychopharmacology 39 (1), 202–219.

Braver, T.S., Barch, D.M., Gray, J.R., Molfese, D.L., Snyder, A., 2001. Anterior cingulate cortex and response conflict: effects of frequency, inhibition and errors. Cereb. Cortex 11 (9), 825–836.

Brown, M.R., Lebel, R.M., Dolcos, F., Wilman, A.H., Silverstone, P.H., Pazderka, H., Fujiwara, E., Wild, T.C., Carroll, A.M., Hodlevskyy, O., 2012. Effects of emotional context on impulse control. Neuroimage 63 (1), 434–446.

Chase, H.W., Eickhoff, S.B., Laird, A.R., Hogarth, L., 2011. The neural basis of drug stimulus processing and craving: an activation likelihood estimation meta-analysis. Biol. Psychiatry 70 (8), 785–793.

Chester, D.S., Lynam, D.R., Milich, R., Powell, D.K., Andersen, A.H., DeWall, C.N., 2016. How do negative emotions impair self-control? A neural model of negative urgency. NeuroImage 132, 43–50.

Chikazoe, J., Konishi, S., Asari, T., Jimura, K., Miyashita, Y., 2007. Activation of right inferior frontal gyrus during response inhibition across response modalities. J. Cogn. Neurosci. 19 (1), 69–80.

Corbetta, M., Patel, G., Shulman, G.L., 2008. The reorienting system of the human brain: from environment to theory of mind. Neuron 58 (3), 306–324.

Crawford, J.R., Henry, J.D., 2004. The positive and negative affect schedule (PANAS): construct validity, measurement properties and normative data in a large non-clinical sample. Br. J. Clin. Psychol. 43 (3), 245–265.

Curci, A., Lanciano, T., Soleti, E., Rimé, B., 2013. Negative emotional experiences arouse rumination and affect working memory capacity. Emotion 13 (5), 867.

Cyders, M.A., Coskunpinar, A., 2011. Measurement of constructs using self-report and behavioral lab tasks: is there overlap in nomothetic span and construct representation for impulsivity? Clin. Psychol. Rev. 31 (6), 965–982.

Cyders, M.A., Smith, G.T., 2008. Emotion-based dispositions to rash action: positive and negative urgency. Psychol. Bull. 134 (6), 807.

Czapla, M., Simon, J.J., Friederich, H.-C., Herpertz, S.C., Zimmermann, P., Loeber, S., 2015. Is binge drinking in young adults associated with an alcohol-specific impairment of response inhibition? Eur. Addict. Res. 21 (2), 105–113.

Czapla, M., Baeuchl, C., Simon, J.J., Richter, B., Kluge, M., Friederich, H.-C., Mann, K., Herpertz, S.C., Loeber, S., 2017. Do alcohol-dependent patients show different neural activation during response inhibition than healthy controls in an alcohol-related fMRI go/no-go-task? Psychopharmacology 234 (6), 1001–1015.

Dean, A.C., Nurmi, E.L., Moeller, S.J., Amir, N., Rozenman, M., Ghahremani, D.G., Johnson, M., Berberyan, R., Hellemann, G., Zhang, Z., 2019. No effect of attentional bias modification training in methamphetamine users receiving residential treatment. Psychopharmacology 236 (2), 709–721.

Dickerson, B.C., Eichenbaum, H., 2010. The episodic memory system: neurocircuitry and disorders. Neuropsychopharmacology 35 (1), 86–104.

Dong, G., DeVito, E.E., Du, X., Cui, Z., 2012. Impaired inhibitory control in 'internet addiction disorder': a functional magnetic resonance imaging study. Psychiatry Res.: Neuroimaging 203 (2–3), 153–158.

Duann, J.-R., Ide, J.S., Luo, X., Li, C.-sr., 2009. Functional connectivity delineates distinct roles of the inferior frontal cortex and presupplementary motor area in stop signal inhibition. J. Neurosci. 29 (32), 10171–10179.

Ekhtiari, H., Alam-Mehrjerdi, Z., Nouri, M., George, S., Mokri, A., 2010. Designing and evaluation of reliability and validity of visual cue-induced craving assessment task for methamphetamine smokers. Basic Clin. Neurosci. 1 (4), 34–37.

Ekhtiari, H., Kuplicki, R., Pruthi, A., Paulus, M., 2020. Methamphetamine and opioid cue database (MOCD): development and validation. Drug Alcohol Depend. 209, 107941.

Ekhtiari, H., Zare-Bidoky, M., Verdejo-Garcia, A., 2021. Neurocognitive disorders in substance use disorders. Textbook of Addiction Treatment. Springer, pp. 1159–1176.

Fan, L., Li, H., Zhuo, J., Zhang, Y., Wang, J., Chen, L., Yang, Z., Chu, C., Xie, S., Laird, A. R., 2016. The human brainnetome atlas: a new brain atlas based on connectional architecture. Cereb. Cortex 26 (8), 3508–3526.

Garavan, H., Ross, T., Stein, E., 1999. Right hemispheric dominance of inhibitory control: an event-related functional MRI study. Proc. Natl. Acad. Sci. USA 96 (14), 8301–8306.

Garavan, H., Pankiewicz, J., Bloom, A., Cho, J.-K., Sperry, L., Ross, T.J., Salmeron, B.J., Risinger, R., Kelley, D., Stein, E.A., 2000. Cue-induced cocaine craving: neuroanatomical specificity for drug users and drug stimuli. Am. J. Psychiatry 157 (11), 1789–1798.

Garavan, H., Ross, T.J., Murphy, K., Roche, R.A., Stein, E.A., 2002. Dissociable executive functions in the dynamic control of behavior: inhibition, error detection, and correction. Neuroimage 17 (4), 1820–1829.

Garrison, K.A., Potenza, M.N., 2014. Neuroimaging and biomarkers in addiction treatment. Curr. Psychiatry Rep. 16 (12), 513.

Gilman, J.M., Radoman, M., Schuster, R.M., Pachas, G., Azzouz, N., Fava, M., Evins, A.E., 2018. Anterior insula activation during inhibition to smoking cues is associated with ability to maintain tobacco abstinence. Addict. Behav. Rep. 7, 40–46.

Goldstein, M., Brendel, G., Tuescher, O., Pan, H., Epstein, J., Beutel, M., Yang, Y., Thomas, K., Levy, K., Silverman, M., 2007. Neural substrates of the interaction of emotional stimulus processing and motor inhibitory control: an emotional linguistic go/no-go fMRI study. Neuroimage 36 (3), 1026–1040.

Goldstein, R.Z., Volkow, N.D., 2002. Drug addiction and its underlying neurobiological basis: neuroimaging evidence for the involvement of the frontal cortex. Am. J. Psychiatry 159 (10), 1642–1652.

Goldstein, R.Z., Volkow, N.D., 2011. Dysfunction of the prefrontal cortex in addiction: neuroimaging findings and clinical implications. Nat. Rev. Neurosci. 12 (11), 652–669.

Grodin, E.N., Courtney, K.E., Ray, L.A., 2019. Drug-induced craving for methamphetamine is associated with neural methamphetamine Cue reactivity. J. Stud. Alcohol Drugs 80 (2), 245–251.

Gruber, S.A., Yurgelun-Todd, D.A., 2005. Neuroimaging of marijuana smokers during inhibitory processing: a pilot investigation. Cogn. Brain Res. 23 (1), 107–118.

Grüsser, S.M., Wrase, J., Klein, S., Hermann, D., Smolka, M.N., Ruf, M., Weber-Fahr, W., Flor, H., Mann, K., Braus, D.F., 2004. Cue-induced activation of the striatum and medial prefrontal cortex is associated with subsequent relapse in abstinent alcoholics. Psychopharmacology 175 (3), 296–302.

Guterstam, J., Jayaram-Lindström, N., Berrebi, J., Petrovic, P., Ingvar, M., Fransson, P., Franck, J., 2018. Cue reactivity and opioid blockade in amphetamine dependence: a randomized, controlled fMRI study. Drug Alcohol Depend. 191, 91–97.

Hampshire, A., Chamberlain, S.R., Monti, M.M., Duncan, J., Owen, A.M., 2010. The role of the right inferior frontal gyrus: inhibition and attentional control. Neuroimage 50 (3), 1313–1319.

Hanlon, C.A., Dowdle, L.T., Gibson, N.B., Li, X., Hamilton, S., Canterberry, M., Hoffman, M., 2018. Cortical substrates of cue-reactivity in multiple substance dependent populations: transdiagnostic relevance of the medial prefrontal cortex. Transl. Psychiatry 8 (1), 1–8.

Heatherton, T.F., Wagner, D.D., 2011. Cognitive neuroscience of self-regulation failure. Trends Cogn. Sci. 15 (3), 132–139.

Hedegaard, H., Bastian, B.A., Trinidad, J.P., Spencer, M., Warner, M., 2018. Drugs most frequently involved in drug overdose deaths: United States, 2011–2016.

Jan, R.K., Kydd, R.R., Russell, B.R., 2012. Functional and structural brain changes associated with methamphetamine abuse. Brain Sci. 2 (4), 434–482.

Johnson, S.L., Elliott, M.V., Carver, C.S., 2020. Impulsive responses to positive and negative emotions: parallel neurocognitive correlates and their implications. Biol. Psychiatry 87 (4), 338–349.

Jones, A., Robinson, E., Duckworth, J., Kersbergen, I., Clarke, N., Field, M.J.A., 2018. The effects of exposure to appetitive cues on inhibitory control: a meta-analytic investigation. Appetite 128, 271–282.

Kaiser, A.J., Milich, R., Lynam, D.R., Charnigo, R.J., 2012. Negative urgency, distress tolerance, and substance abuse among college students. Addict. Behav. 37 (10), 1075–1083.

Kelly, A.C., Hester, R., Murphy, K., Javitt, D.C., Foxe, J.J., Garavan, H., 2004. Prefrontal-subcortical dissociations underlying inhibitory control revealed by event-related fMRI. Eur. J. Neurosci. 19 (11), 3105–3112.

Kreusch, F., Vilenne, A., Quertemont, E., 2013. Response inhibition toward alcohol-related cues using an alcohol go/no-go task in problem and non-problem drinkers. Addict. Behav. 38 (10), 2520–2528.

Kühn, S., Gallinat, J., 2011. Common biology of craving across legal and illegal drugs–a quantitative meta-analysis of cue-reactivity brain response. Eur. J. Neurosci. 33 (7), 1318–1326.

Kwako, L.E., Momenan, R., Grodin, E.N., Litten, R.Z., Koob, G.F., Goldman, D.J.N., 2017. Addictions neuroclinical assessment: a reverse translational approach. 122, 254–264.

Lang, P.J., Bradley, M.M., Cuthbert, B.N., 1997. International affective picture system (IAPS): Technical manual and affective ratings, 1. NIMH Center for the Study of Emotion and Attention, pp. 39–58.

Lannoy, S., Dormal, V., Billieux, J., Brion, M., D'Hondt, F., Maurage, P., 2019. A dual-process exploration of binge drinking: evidence through behavioral and electrophysiological findings. Fr. J. Psychiatry 1, S92.

Liddle, P.F., Kiehl, K.A., Smith, A.M., 2001. Event-related fMRI study of response inhibition. Hum. Brain Mapp. 12 (2), 100–109.

Liu, G.-C., Yen, J.-Y., Chen, C.-Y., Yen, C.-F., Chen, C.-S., Lin, W.-C., Ko, C.-H., 2014. Brain activation for response inhibition under gaming cue distraction in internet gaming disorder. Kaohsiung J. Med. Sci. 30 (1), 43–51.

Luijten, M., Machielsen, M.W., Veltman, D.J., Hester, R., de Haan, L., Franken, I.H., 2014. Systematic review of ERP and fMRI studies investigating inhibitory control and error processing in people with substance dependence and behavioural addictions. J. Psychiatry Neurosci.

Luijten, M., Schellekens, A.F., Kühn, S., Machielse, M.W., Sescousse, G., 2017. Disruption of reward processing in addiction: an image-based meta-analysis of functional magnetic resonance imaging studies. JAMA Psychiatry 74 (4), 387–398.

Mathalon, D.H., Whitfield, S.L., Ford, J.M., 2003. Anatomy of an error: ERP and fMRI. Biol. Psychol. 64 (1–2), 119–141.
May, A.C., Aupperle, R.L., Stewart, J.L., 2020. Dark times: the role of negative reinforcement in methamphetamine addiction. Front. Psychiatry 11.
McNab, F., Leroux, G., Strand, F., Thorell, L., Bergman, S., Klingberg, T., 2008. Common and unique components of inhibition and working memory: an fMRI, within-subjects investigation. Neuropsychologia 46 (11), 2668–2682.
Monterosso, J.R., Aron, A.R., Cordova, X., Xu, J., London, E.D., 2005. Deficits in response inhibition associated with chronic methamphetamine abuse. Drug Alcohol Depend. 79 (2), 273–277.
Mostofsky, S.H., Simmonds, D.J., 2008. Response inhibition and response selection: two sides of the same coin. J. Cogn. Neurosci. 20 (5), 751–761.
Mostofsky, S.H., Schafer, J.G., Abrams, M.T., Goldberg, M.C., Flower, A.A., Boyce, A., Courtney, S.M., Calhoun, V.D., Kraut, M.A., Denckla, M.B., 2003. fMRI evidence that the neural basis of response inhibition is task-dependent. Cogn. Brain Res. 17 (2), 419–430.
Naqvi, N.H., Bechara, A., 2009. The hidden island of addiction: the insula. Trends Neurosci. 32 (1), 56–67.
Nestor, L.J., Ghahremani, D.G., Monterosso, J., London, E.D., 2011. Prefrontal hypoactivation during cognitive control in early abstinent methamphetamine-dependent subjects. Psychiatry Res.: Neuroimaging 194 (3), 287–295.
Noël, X., Van der Linden, M., d'Acremont, M., Bechara, A., Dan, B., Hanak, C., Verbanck, P., 2007. Alcohol cues increase cognitive impulsivity in individuals with alcoholism. Psychopharmacology 192 (2), 291–298.
Novick, J.M., Trueswell, J.C., Thompson-Schill, S.L., 2005. Cognitive control and parsing: reexamining the role of Broca's area in sentence comprehension. Cogn. Affect. Behav. Neurosci. 5 (3), 263–281.
Oldfield, R.C., 1971. The assessment and analysis of handedness: the Edinburgh inventory. Neuropsychologia 9 (1), 97–113.
Osman, D., Buchon, N., Chakrabarti, S., Huang, Y.-T., Su, W.-C., Poidevin, M., Tsai, Y.-C., Lemaitre, B., 2012. Autocrine and paracrine unpaired signaling regulate intestinal stem cell maintenance and division. J. Cell Sci. 125 (24), 5944–5949.
Ott, T., Nieder, A., 2019. Dopamine and cognitive control in prefrontal cortex. Trends Cogn. Sci. 23 (3), 213–234.
Paulus, M.P., Stewart, J.L., 2020. Neurobiology, clinical presentation, and treatment of methamphetamine use disorder: a review. JAMA Psychiatry 77 (9), 959–966.
Paulus, M.P., Tapert, S.F., Schuckit, M.A., 2005. Neural activation patterns of methamphetamine-dependent subjects during decision making predict relapse. Arch. Gen. Psychiatry 62 (7), 761–768.
Qiu, Z., Wang, J., 2021. Altered neural activities during response inhibition in adults with addiction: a voxel-wise meta-analysis. Psychol. Med. 51 (3), 387–399.
R Core Team, R., 2013. R: A language and environment for statistical computing. R foundation for statistical computing Vienna, Austria.
Ramos-Loyo, J., Llamas-Alonso, L.A., González-Garrido, A.A., Hernández-Villalobos, J., 2017. Emotional contexts exert a distracting effect on attention and inhibitory control in female and male adolescents. Sci. Rep. 7 (1), 1–10.
Reuter, J., Raedler, T., Rose, M., Hand, I., Gläscher, J., Büchel, C., 2005. Pathological gambling is linked to reduced activation of the mesolimbic reward system. Nat. Neurosci. 8 (2), 147–148.
Sabrini, S., Wang, G.Y., Lin, J.C., Ian, J., Curley, L.E., 2019. Methamphetamine use and cognitive function: a systematic review of neuroimaging research. Drug Alcohol Depend. 194, 75–87.
Seok, J.-w, Sohn, J.-H., 2020. Response inhibition during processing of sexual stimuli in males with problematic hypersexual behavior. J. Behav. Addict. 9 (1), 71–82.
Shenhav, A., Botvinick, M.M., Cohen, J.D., 2013. The expected value of control: an integrative theory of anterior cingulate cortex function. Neuron 79 (2), 217–240.
Simmonds, D.J., Pekar, J.J., Mostofsky, S.H., 2008. Meta-analysis of Go/No-go tasks demonstrating that fMRI activation associated with response inhibition is task-dependent. Neuropsychologia 46 (1), 224–232.
Stein, M., Steiner, L., Fey, W., Conring, F., Rieger, K., Federspiel, A., Moggi, F., 2021. Alcohol-related context modulates neural correlates of inhibitory control in alcohol dependent patients: preliminary data from an fMRI study using an alcohol-related Go/NoGo-task. Behav. Brain Res. 398, 112973.
Su, B., Li, S., Yang, L., Zheng, M.J.P., 2020. Reduced response inhibition after exposure to drug-related cues in male heroin abstainers. 237(4), 1055–1062.
Swick, D., Ashley, V., Turken, U., 2008. Left inferior frontal gyrus is critical for response inhibition. BMC Neurosci. 9 (1), 1–11.
Swick, D., Ashley, V., Turken, U., 2011. Are the neural correlates of stopping and not going identical? Quantitative meta-analysis of two response inhibition tasks. Neuroimage 56 (3), 1655–1665.
Tang, D., Fellows, L., Small, D., Dagher, A., 2012. Food and drug cues activate similar brain regions: a meta-analysis of functional MRI studies. Physiol. Behav. 106 (3), 317–324.
Tapert, S.F., Schweinsburg, A.D., Drummond, S.P., Paulus, M.P., Brown, S.A., Yang, T.T., Frank, L.R., 2007. Functional MRI of inhibitory processing in abstinent adolescent marijuana users. Psychopharmacology 194 (2), 173–183.
Um, M., Whitt, Z.T., Revilla, R., Hunton, T., Cyders, M.A., 2019. Shared neural correlates underlying addictive disorders and negative urgency. Brain Sci. 9 (2), 36.
United Nations Office on Drugs and Crime, 2018. World Drug Report 2018 (set of 5 Booklets). UN.
van Holst, R.J., van der Meer, J.N., McLaren, D.G., van den Brink, W., Veltman, D.J., Goudriaan, A.E., 2012. Interactions between affective and cognitive processing systems in problematic gamblers: a functional connectivity study. PLOS One 7 (11), e49923.
Wager, T.D., Sylvester, C.-Y.C., Lacey, S.C., Nee, D.E., Franklin, M., Jonides, J., 2005. Common and unique components of response inhibition revealed by fMRI. Neuroimage 27 (2), 323–340.
Weafer, J., Fillmore, M.T., 2012. Alcohol-related stimuli reduce inhibitory control of behavior in drinkers. Psychopharmacology 222 (3), 489–498.
Xu, X., Yuan, H., Lei, X., 2016. Activation and connectivity within the default mode network contribute independently to future-oriented thought. Sci. Rep. 6 (1), 1–10.
Yeung, M.K., Tsuchida, A., Fellows, L.K., 2020. Causal prefrontal contributions to stop-signal task performance in humans. J. Cogn. Neurosci. 1–14.
Yin, J.-J., Ma, S.-H., Xu, K., Wang, Z.-X., Le, H.-B., Huang, J.-Z., Fang, K.-M., Liao, L.-M., Cai, Z.-L., 2012. Functional magnetic resonance imaging of methamphetamine craving. Clin. Imaging 36 (6), 695–701.
Yücel, M., Oldenhof, E., Ahmed, S.H., Belin, D., Billieux, J., Bowden-Jones, H., Carter, A., Chamberlain, S.R., Clark, L., Connor, J., 2019. A transdiagnostic dimensional approach towards a neuropsychological assessment for addiction: an international Delphi consensus study. Addiction 114 (6), 1095–1109.
Zilverstand, A., Huang, A.S., Alia-Klein, N., Goldstein, R.Z., 2018. Neuroimaging impaired response inhibition and salience attribution in human drug addiction: a systematic review. Neuron 98 (5), 886–903.